

1

2

3

4 **Modulation of anti-tumor immunity**  
5 **by the brain's reward system**

6

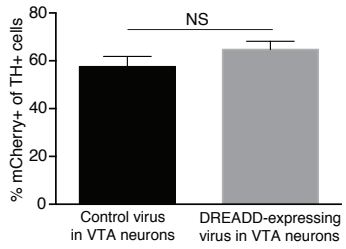
7

**Ben-Shaanan, Schiller et al.**

8

9

10 **Supplementary Figure legends:**  
11

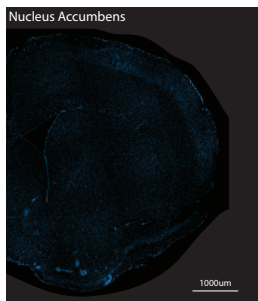
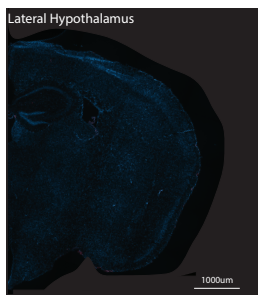
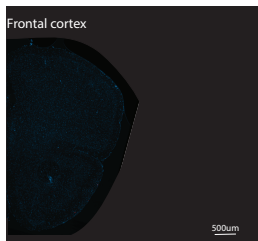


12

13 **Supplementary Fig. 1**

14 **Efficiency of viral expression in the VTA dopaminergic neurons.** Immunohistochemical  
15 analysis represented as percentage of mCherry positive cells of all TH<sup>+</sup> cells in the VTA of mice  
16 stereotactically injected with a virus carrying a gene encoding the DREADD receptor, or a control  
17 virus (encoding only the expression of the fluorescent reporter, mCherry). ( $P < 0.26$ ; Student's *t*-  
18 *test*; mean  $\pm$  s.e.m; n = 3).

19



20



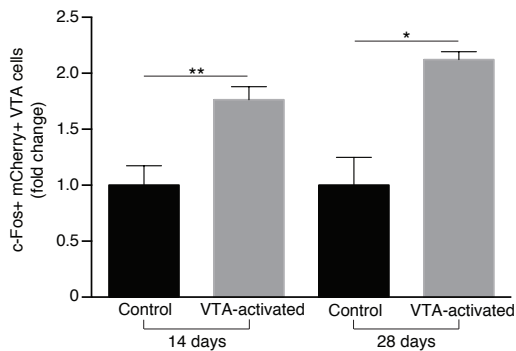
21 **Supplementary Fig. 2**

22 **Lack of mCherry expression in the Nucleus Accumbens, Lateral Hypothalamus and Frontal**  
23 **Cortex.** Representative images taken from mice stereotactically injected with virus in the VTA  
24 region, showing lack of neuronal expression of the fluorescent reporter mCherry in the Frontal  
25 Cortex, Lateral Hypothalamus and Nucleus Accumbens. DAPI staining is provided for  
26 visualization (mCherry- red; Dapi- blue).

27

28

29



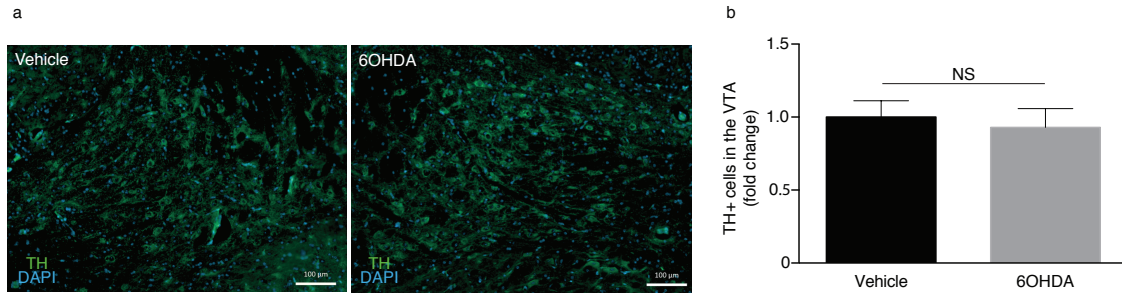
30

31 **Supplementary Fig. 3**

32 **DREADD manipulation increases percentage of c-Fos positive neurons in the VTA.**  
33 Quantitative immunohistochemical analysis of the percent of c-Fos expressing cells among  
34 DREADD-expressing VTA neurons following 14 or 28 days of CNO injections (for 14 days  
35  $P < 0.005$ , for 28 days  $P < 0.012$ ; Student's *t*-test; mean  $\pm$  s.e.m; n= 6, 3). Data are presented as mean  
36 fold change in c-Fos expression in mCherry positive neurons relative to the controls expressing the  
37 sham virus, and treated with CNO.

38

39



40

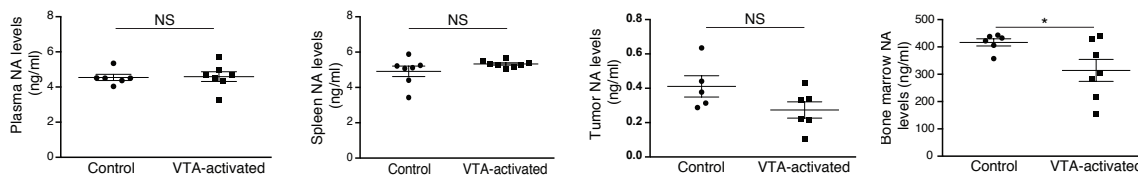
41 **Supplementary Fig. 4**

42 **6OHDA treatment does not affect the number of TH<sup>+</sup> neurons in the VTA of tumor-bearing**  
 43 **mice** (a) Representative immunohistochemical staining image of the VTA region from mice treated  
 44 with 6OHDA and vehicle, stained for Tyrosine Hydroxylase (TH; green) and DAPI (blue). (b)  
 45 Quantitative immunohistochemical analysis of the number of TH<sup>+</sup> cells in the same VTA area  
 46 (mm<sup>2</sup>) of mice treated with 6OHDA versus vehicle ( $p < 0.69$ ; Student's *t*-test; NS- not significant;  
 47  $n = 4$ ). Data is presented as mean fold change relative to the control group average  $\pm$  s.e.m.

48

49

50

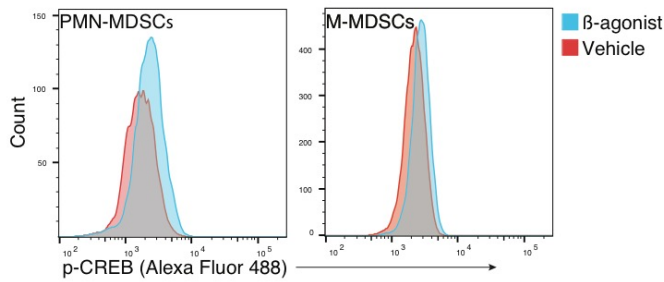


51 **Supplementary Fig. 5**

52 **The effects of VTA-activation on noradrenaline levels in the plasma, spleen, tumor and bone**  
 53 **marrow.** Quantitative ELISA analysis of noradrenaline levels in the plasma, spleen, tumor and  
 54 bone marrow of tumor-bearing mice, following daily VTA activation for 14 days. Controls were  
 55 injected with a control virus and treated with CNO. (for plasma  $P < 0.893$  and  $n = 6, 7$ ; spleen  $P < 0.16$   
 56 and  $n = 7, 8$ ; tumor  $P < 0.107$  and  $n = 5, 6$ ; bone marrow  $P < 0.044$  and  $n = 6, 7$ ; Student's *t*-test;  
 57 mean  $\pm$  s.e.m; NS-not significant). Data represent two independent repeats

58

59



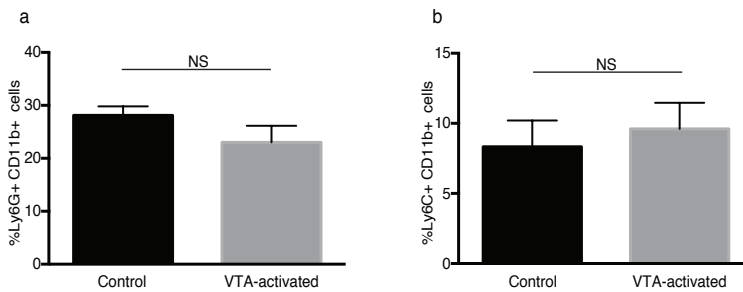
60

61 **Supplementary Fig. 6**

62 **Representative histograms of p-CREB staining in bone marrow MDSCs.** The populations  
 63 shown in the histograms are PMN-MDSCs (CD11b<sup>+</sup> Gr-1<sup>+</sup> Ly6G<sup>+</sup>) and M-MDSCs (CD11b<sup>+</sup> Gr-1<sup>+</sup>  
 64 Ly6C<sup>+</sup>). The X axis represents p-CREB levels.

65

66



67

68

69 **Supplementary Fig. 7**

70 **VTA activation does not affect the relative abundance of tumor PMN-MDSCs and M-**  
 71 **MDSCs.** Flow cytometry analysis of (a) PMN-MDSCs (Gr-1<sup>+</sup> CD11b<sup>+</sup> LY6G<sup>+</sup>) and (b) M-MDSCs  
 72 (Gr-1<sup>+</sup> CD11b<sup>+</sup> LY6C<sup>+</sup>) abundance out of all tumor cells from mice subjected to daily VTA  
 73 activation for 14 days, and their controls. (PMN-MDSCs  $P < 0.22$ ,  $n = 6, 8$ ; M-MDSCs  $P < 0.64$ ,  $n = 6,$   
 74  $7$ ; Student's *t*-test; NS-not significant). Data represent two independent repeats.

75

76

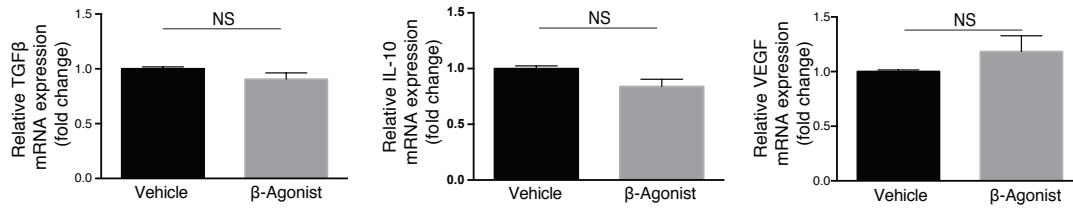
77

78

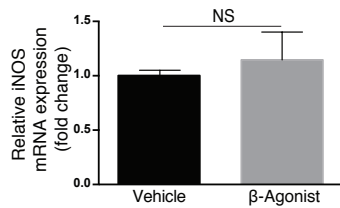
79

80

81



82



83

84 **Supplementary Fig. 8**

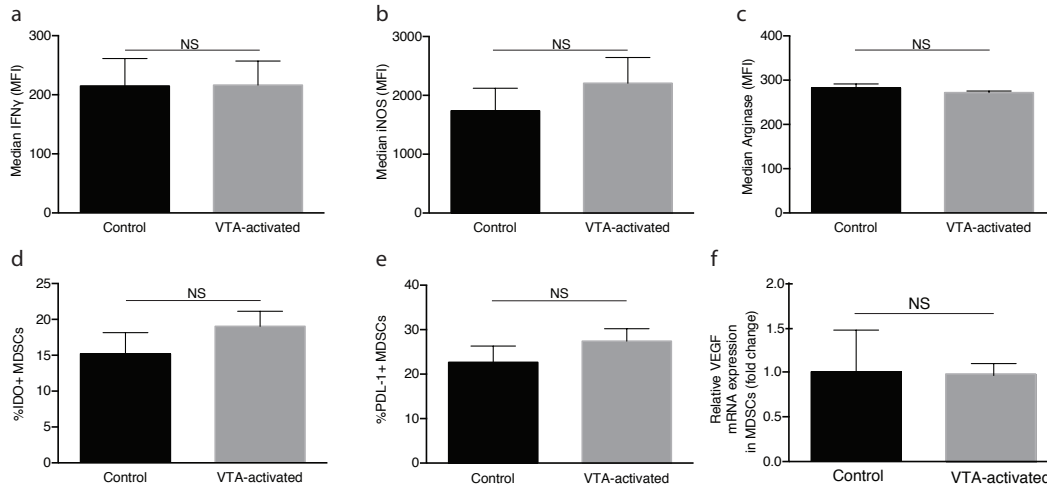
85 **Effects of β-adrenergic agonist on bone marrow MDSCs mRNA expression of TGFβ, IL-10,**  
86 **VEGF, and iNOS.** qPCR analysis of TGFβ, IL-10, VEGF and iNOS mRNA expression levels by  
87 MDSCs (Gr-1<sup>+</sup>CD11b<sup>+</sup>) sorted from the bone marrow of tumor-bearing mice, and incubated *in-*  
88 *vitro* with the β-adrenergic agonist (isoproterenol 1uM; TGFβ  $P<0.22$ , IL-10  $P<0.09$ , VEGF  
89  $P<0.66$ , iNOS  $P<0.94$ ; Mann-Whitney test to account for the multiple comparisons; NS- not  
90 significant; n=5). \* $P<0.1$ .

91

92

93

94



95

96

97

98 **Supplementary Fig. 9**

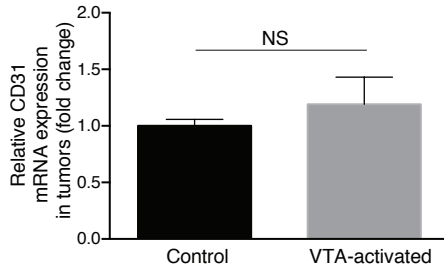
99 **Characterization of MDSCs isolated from VTA-activated and control mice.** Tumor MDSCs  
 100 expression of (a) IFN $\gamma$ , (b) iNOS, (c) Arginase, (d) IDO-1 and (e) PDL-1 from VTA-activated mice  
 101 and their controls (injected with a control virus and treated with CNO) using flow cytometry. For  
 102 IFN $\gamma$ , iNOS and Arginase, the data represent mean  $\pm$  s.e.m of median marker expression among  
 103 tumor MDSCs from VTA-activated mice and their controls. For IDO-1 and PD-1, the data represent  
 104 mean  $\pm$  s.e.m of the abundance of marker-positive MDSCs from VTA-activated mice and their  
 105 controls. (f) mRNA levels of VEGF expressed by MDSCs from VTA activated mice and their  
 106 controls were analyzed by qPCR. (IFN $\gamma$  analysis  $p < 0.98$  and  $n = 8$ ; iNOS analysis  $p < 0.44$  and  
 107  $n = 8, 10$ ; for IDO-1  $p < 0.35$  and  $n = 5, 4$ ; for PD-1  $p < 0.36$  and  $n = 5, 4$ ; for Arginase  $p < 0.34$  and  $n = 5, 4$ ;  
 108 VEGF analysis  $p < 0.95$  and  $n = 4, 7$ ; Student's *t*-test; NS-not significant).

109

110

111

112



113

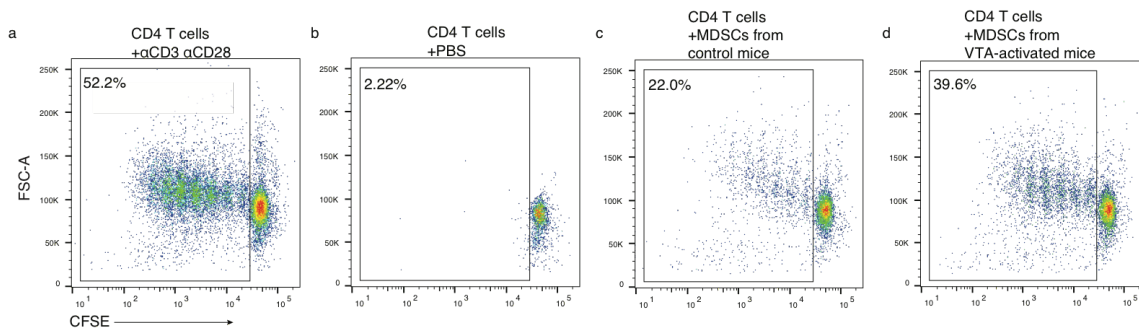
114 **Supplementary Fig. 10**

115 **VTA activation does not affect tumor mRNA expression of CD31.** Tumors from VTA-  
 116 activated mice and their controls were analyzed for CD31 levels by qPCR ( $p < 0.41$ ; Student's *t*-  
 117 test; NS-not significant; n=4,3).

118

119

120



121

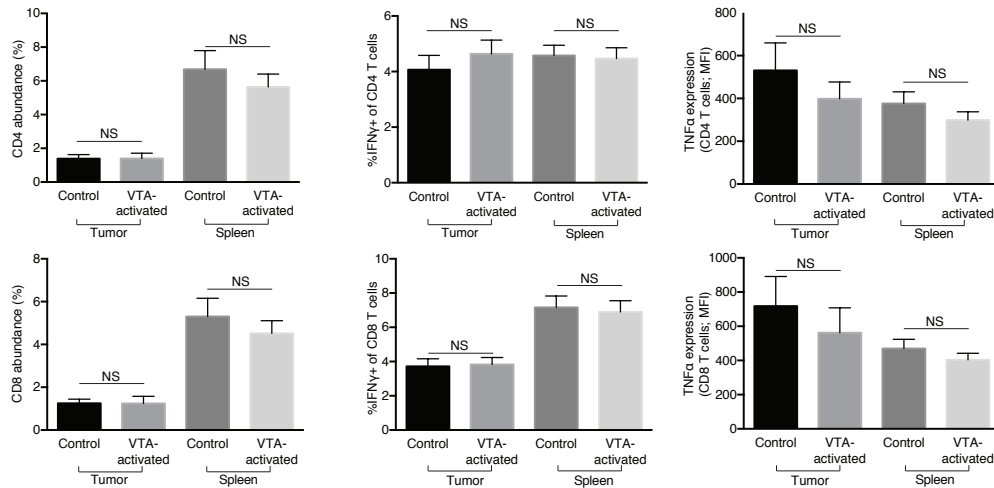
122

123

124 **Supplementary Fig. 11**

125 **Representative dot-plots for MDSCs-suppression assay.** CFSE labelled CD4 T cells were  
 126 incubated under the following conditions: (a) Stimulated with anti CD3 and anti CD28 in culture  
 127 medium, (b) incubated in culture medium in the absence of stimulating signals, (c) stimulated with  
 128 anti CD3 and anti CD28 in the presence of MDSCs isolated from sham-virus injected mice, (d)  
 129 stimulated with anti CD3 and anti CD28 in the presence of MDSCs isolated from VTA-activated  
 130 mice. Cells were analyzed after 96hr incubation. The percent suppression of proliferating T cells  
 131 was calculated as described in the methods.

132



133  
134

135 **Supplementary Fig. 12**

136 **VTA activation does not affect tumor and spleen CD4 and CD8 cell abundance, nor IFN $\gamma$  and**  
 137 **TNF $\alpha$  expression.** Flow cytometry analysis of tumor and spleen CD4 (TCR $\beta^+$  CD4 $^+$ ) and CD8 T  
 138 cell (TCR $\beta^+$  CD8 $^+$  CD49b $^-$ ) abundance, and expression of IFN $\gamma$  and TNF $\alpha$  following repeated  
 139 VTA-activation. (CD4 tumor cells abundance ( $P < 0.98$ ), IFN $\gamma^+$  percentage ( $P < 0.44$ ), TNF $\alpha$   
 140 expression ( $P < 0.39$ ),  $n = 7$ ; spleen CD4 cells abundance ( $P < 0.46$ ), IFN $\gamma^+$  percentage ( $P < 0.84$ ),  
 141 TNF $\alpha$  expression ( $P < 0.29$ ),  $n = 8, 7$ ; CD8 tumor cells abundance ( $P < 0.99$ ), IFN $\gamma^+$  percentage  
 142 ( $P < 0.85$ ) and TNF $\alpha$  expression ( $P < 0.50$ ),  $n = 7$ ; spleen CD8 cells abundance ( $P < 0.47$ ), IFN $\gamma^+$   
 143 percentage ( $P < 0.78$ ) and TNF $\alpha$  expression ( $P < 0.37$ ),  $n = 8, 7$ ; Student's *t*-test; mean  $\pm$  s.e.m; NS-  
 144 not significant).

145

146

147

148

149

150

151

152

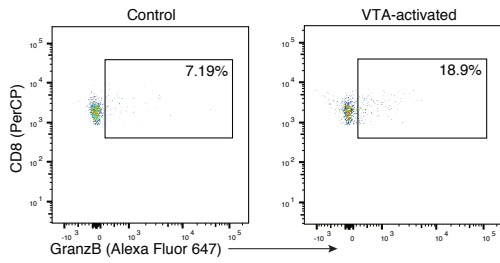
153

154

155

156

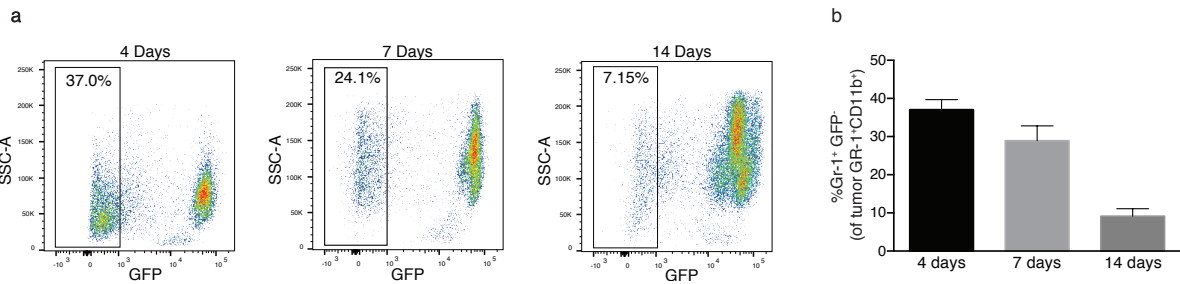
157



158  
159  
160  
161  
162  
163  
164  
165  
166  
167  
168

**Supplementary Fig. 13**

**Representative dot plots of Granzyme B expression by tumor CD8 T cells from VTA activated and control mice.** Representative dot plots show gated tumor CD8 T cells identified by TCR $\beta^+$  CD8 $^+$  CD49b $^-$ . X axis represents Granzyme B expression, while the Y axis represents CD8 expression.



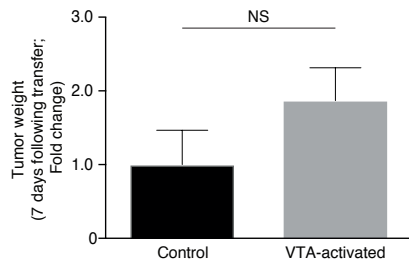
169  
170  
171  
172  
173  
174  
175  
176  
177  
178  
179  
180

**Supplementary Fig. 14**

**Evaluation of transferred MDSCs survival in tumor-bearing GFP mice.**

transferred from tumor-bearing mice into GFP mice, along with LLC tumor cells. (a) Representative images and (b) Quantification of transferred MDSCs (identified as GFP $^-$  CD11b $^+$  Gr-1 $^+$ ). Their abundance was analyzed at 4,7 and 14 days after transfer out of total CD11b $^+$  Gr-1 $^+$  cells in tumor (for 4 days n=4; for 7 days n=4; for 14 days n=2; Student's *t-test*; mean  $\pm$  s.e.m).





181  
182

183 **Supplementary Fig. 15**

184 **Transfer of MDSCs from VTA-activated mice and their controls along with naïve tumor cells**  
185 **does not affect tumor weight 7 days following transfer.** MDSCs were isolated from VTA-  
186 activated mice and their controls. The cells were then co-injected along with new tumor cells into  
187 naïve recipient mice. The recipient mice were injected with an equal number of MDSCs and LLC  
188 cells. To ensure that there is a detectable tumor at this early time point, we injected a larger number  
189 of MDSCs and tumor cells, preserving the original ratio between the two cell types ( $1 \times 10^6$  of each  
190 cell type). Data is shown as fold change relative to the average of the control group ( $P < 0.24$ ;  
191 Student's *t*-test; mean  $\pm$  s.e.m; NS-not significant; n=3, 4).

192  
193